SAE 00160

An analytical approach for discrete controllers design using a new S-Z mapping with two tuning parameters

Marcelo R. A.C. Tredinnick
TechNit RT – Technologies, and PUC-RJ: Pontific Catholic University from Rio de Janeiro. Department of Electronic Engineering. Rua Otávio Carneiro, 100; 1112/1113. Icaraí, Niterói – Rio de Janeiro - Brasil – CEP 24230-190. tredi@osite.com.br.

Marcelo Lopes de O. e Souza
Luiz C. Gadelha de Souza
INPE: National Institute for Space Research / DMC: Space Mechanics and Control Division. Av. dos Astronautas, 1758, CEP: 12201-970, Jardim da Granja. São José dos Campos – SP – Brasil. marcelo@dem.inpe.br / gadelha@dem.inpe.br.

ABSTRACT

In this work we present a second s-z mapping (ST2) as an extension of a first one, the s-z mapping (ST1), presented in a previous work done by the authors. In that work, the ST1 mapping used only one tuning parameter (csi) ξ to: 1) map the (asymptotically stable) left half s plane in the interior of the unitary circle in z plane; and 2) attain the asymptotical stabilization of a benchmark harmonic oscillator driven by a PD discrete controller with various sampling periods. In both tests, the ST1 mapping behaved better than other mappings listed in the literature (Tustin, Backward, Shneider-Kaneshige-Groutage, etc.). In this work we use two tuning parameters csi1 and csi2 in the ST2 mapping to see how both tests behave, including numerical simulations comparing the ST2 mapping with those other mappings ((ST1 and Tustin). Through the numerical results obtained in this work we may perceive that the two new-rules presented are more robust to the fading effects due the increasing of aliasing phenomenon in comparison with the Tustin rule. An analytical description of these new-rules is presented.

INTRODUCTION

Nowadays more and more space mission involves Large Space Structures (LSS)[17], an update example is the International Space Station construction which creates new demands on dynamics techniques where the coupling between the rigid and flexible motion must be take into account in the control system design [15], as well as the interaction between the control system and the flexible structure motion play an important rule in the control system performance [16].

A rigid-flexible structure may be understood [18] [13] as a coupling of two parts: the rigid and the flexible bodies. A flexible structure may be described by an infinite sum of simple and damped harmonic oscillators vibrating each one in one specific structural natural frequency. From empirical data [19] these vibration modes have the damping proportional to their values, i.e., a high frequency mode is highly damped and the first frequency modes are less damped. As yet, there is no satisfactory quantitative theory to predict structural damping [19]. A rigid-flexible system could be represented as shown in the figure below [18].

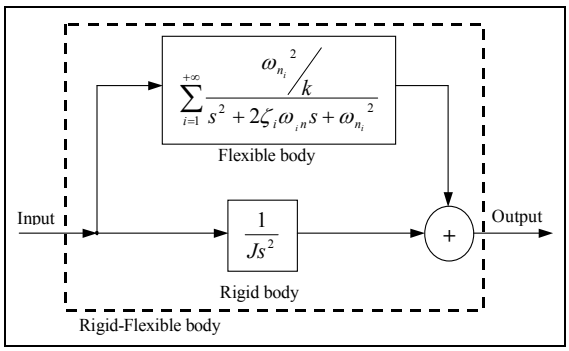

Figure 1– A generic Rigid-Flexible structural system.

As shown in the literature [1] [2], control algorithms can be tested using the simplest configuration for the flexible structure, i.e., analyzing a single harmonic oscillator damped. In the literature [1] [2], the study of stability of a

discrete closed control of a single and damped harmonic oscillator could validate the control algorithm used for a more complex attitude dynamics like an asymmetric rigid-flexible satellite (with 1.4 Ton in rigid-body and 49 kg in the flexible appendage, with a PD control). It is an increasing tendency [17] to employ automatic digital controllers in many industrial and aerospace important applications due its ability of programming, lightweight, less power consumption, and other features. The main objective is the guarantee of the stability first, and the performance analysis after that. When the research about the stability of the discrete closed-loop control about flexible structures will be concluded, we will start the investigations about performance. In the next section we may see an introduction about the benchmark plant used in this work. We have used it in all numerical simulations, using a discrete-time zero-order-hold (ZOH) equivalency [1] [2] [3] [4] [5] [6] [7] [8] [9] [10].

BENCHMARK PLANT USED AND ITS ZOH EQUIVALENCE

In this work we have analyzed and simulated a damped harmonic oscillator given by:

$$\mathrm{m}.\ddot{\mathrm{x}}(\mathrm{t}) + \mathrm{b}.\dot{\mathrm{x}}(\mathrm{t}) + \mathrm{k}.\mathrm{x}(\mathrm{t}) = \mathrm{u}(\mathrm{t}) \qquad \text{(Eq. 1)}$$

Where m is the mass, k is the elasticity factor, and the b is the viscous friction coefficient, with $\mathrm{m} \in (0;\infty)$, $\mathrm{b} \in [0;\mathrm{m})$, $\mathrm{k} \in (0;\infty)$. The analog transfer function are given by:

$$G(s) \overset{\Delta}{=} \frac{X(s)}{U(s)} = \frac{1}{k}.\frac{\omega_n{}^2}{s^2 + 2.\zeta.\omega_n.s + \omega_n{}^2} \qquad \text{(Eq. 2)}$$

where $\omega_n = \sqrt{k/m} \in (0;\infty)$ is the non-damped natural angular frequency of this vibration mode, and $\zeta = \mathrm{b}/\mathrm{m} \in [0;1)$ is its damping ratio.

The zero-order hold (ZOH) equivalent [3] of Eq. 2 may be calculated by:

$$G_{H0}(z) = (1 - z^{-1}).\ Z\left\{ \mathrm{L}^{-1}\left\{ \frac{G(s)}{s} \right\}\Big|_{t=k.T} \right\} \qquad \text{(Eq.3)}$$

Applying Eq. 3 to Eq. 2 we have, after normalizing k=1 we have a second order transfer function with the insertion of a zero due the hold:

$$G_{H0}(z) = \frac{z\left[1 - 2e^{-\sigma T}.\cos(\omega_d T) - e^{-\sigma T}\left(\frac{\sigma}{\omega_d}.\sin(\omega_d T) - \cos(\omega_d T)\right)\right] + e^{-2\sigma T} + e^{-\sigma T}\left(\frac{\sigma}{\omega_d}.\sin(\omega_d T) - \cos(\omega_d T)\right)}{z^2 - [2e^{-\sigma T}.\cos(\omega_d T)]z + e^{-2\sigma T}} \qquad \text{(Eq. 4)}$$

TUSTIN RULE MAPPING

The Tustin rule has the following finite differences equation describing it:

$$e_k = \frac{2}{T}.\nabla u_k - e_{k-1} \qquad \text{(Eq. 5)}$$

$$s \sim \frac{2}{T}.\frac{z-1}{z+1} \qquad \text{(Eq. 6)}$$

Seu mapeamento s-z é dado por:

$$z = \exp\left(j.\tan^{-1}\left[\frac{4\omega T}{4 - (\omega T)^2} \right] \right) \qquad \text{(Eq. 7)}$$

$$\lfloor z \rfloor = 1$$

The equation 7 is describing an unit circle in the z complex space, i.e., all left half plane in s complex space is mapped by Tustin rule (Bilinear) to the interior of this unit circle.

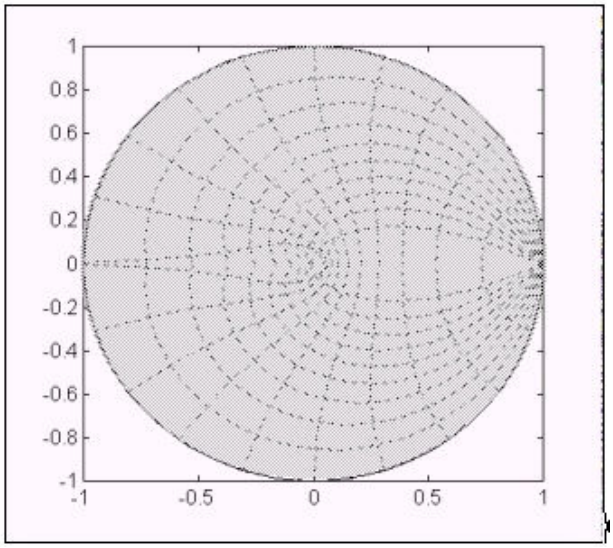

Figure 1– Tustin mapping

NEW-RULE 1 MAPPING (ST1)

The limitations of the classical methods presented so far in preserving the stability for high gains and high sampling periods suggested us to propose new s-z mappings. This begun in two main works in the literature [1] [2] through the difference equation:

$$e_k = \frac{2}{T}.\nabla u_k - \xi.e_{k-1} \qquad \text{(Eq. 8)}$$

Applying the z-transform [3] on it we have the new s-z mapping 1, we will have:

$$s \sim \frac{2}{T}.\frac{z-1}{z+\xi} \qquad ;0 < \xi < 1 \qquad \text{(Eq. 9)}$$

Which shifts the pole from z = -1 in the Tustin rule to z' = -ξ, 0 ≤ ξ ≤ 1. This avoids or retards the instabilization in closed loop systems, by using ξ as a new design parameter

(besides the control gains and the sampling period). The new rule 1 becomes: the Tustin rule if ξ = 1; and the backward mapping if ξ = 0. Its inverse is given by:

$$s = \frac{2}{T}.\frac{z-1}{z+\xi} \quad \Rightarrow \quad z = \frac{2+s.T.\xi}{2-s.T} \qquad (0 \le \xi \le 1) \qquad \text{(Eq.10)}$$

The new rule 1 also maps the left half s plane into a circle with center and radius given by equation 13, always inside the unit circle in plane z. To prove this, note that:

if ξ = 1 → center = 0 ; radius = 1; (Tustin);

if ξ = 0 → center = ½ ; radius = ½; (backward);

The simplest possible expression for the center is:

$$\text{center} = \frac{1}{2}.(1-\xi)$$

(Eq.11)

Lets rewrite equation 7 to describe a circle with center given by equation 11, whose circumference corresponds to s = j.ω:

$$z = \frac{\frac{1}{2}.(1-\xi)[2-j.\omega.T] - \frac{1}{2}.(1-\xi)[2-j.\omega.T] + 2 + j.\omega.T.\xi}{2-j.\omega.T}$$

$$z = \frac{1}{2}.(1-\xi).\frac{[2-j.\omega.T]}{[2-j.\omega.T]} + \frac{-\frac{1}{2}.(1-\xi)[2-j.\omega.T] + 2 + j.\omega.T.\xi}{2-j.\omega.T}$$

$$z - \frac{1}{2}.(1-\xi) = \frac{1+\xi+j.\omega.T.\frac{1}{2}.(1+\xi)}{2-j.\omega.T}$$

$$z - \frac{1}{2}.(1-\xi) = \frac{1}{2}.(1+\xi).\exp\left(j\tan^{-1}\left(\frac{4.\omega.T}{4-(\omega.T)^2}\right)\right) \qquad \text{(Eq.12)}$$

Which proves the thesis. Thus, the equation of the new-rule mapping is described as:

$$\left| z - \frac{1}{2}.(1-\xi) \right| = \frac{1}{2}.(1+\xi)$$

(Eq.13)

We may see the new, the Tustin and the backward mappings graphical comparison at the figure 2.

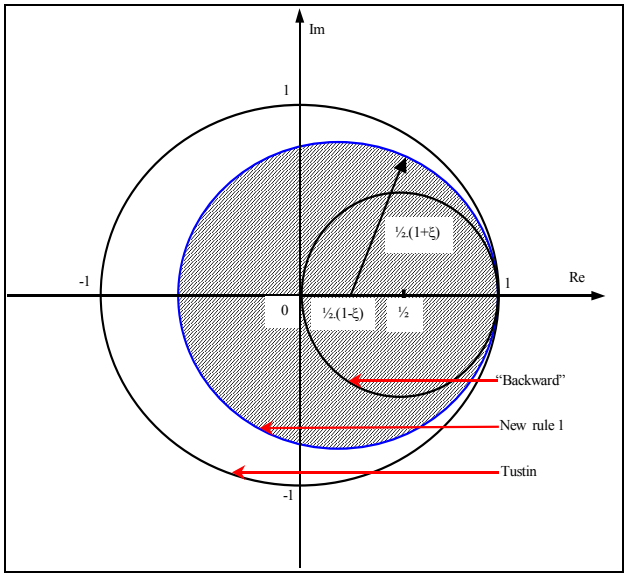

Figure 2 The New-Rule 1, the Tustin and the backward mappings.

NEW-RULE 2 MAPPING (ST2)

The equation of finite differences for the new-rule 2 is:

$$e_k = \frac{2}{T}.(u_k - \xi_1 u_{k-1}) - \xi_2.e_{k-1} \qquad \text{(Eq.14)}$$

Applying the z-transform [3] on it we have the new s-z mapping #2:

$$s \sim \frac{2}{T}.\frac{z-\xi_1}{z+\xi_2} \qquad ;0 < \{\xi_1, \xi_2\} < 1 \qquad \text{(Eq.15)}$$

In analogy to the last case,

$$z = \frac{\frac{1}{2}.(\xi_1-\xi_2)[2-j.\omega.T] - \frac{1}{2}.(\xi_1-\xi_2)[2-j.\omega.T] + 2\xi_1 + j.\omega.T.\xi_2}{2-j.\omega.T}$$

$$z = \frac{1}{2}.(\xi_1-\xi_2).\frac{[2-j.\omega.T]}{[2-j.\omega.T]} + \frac{-\frac{1}{2}.(\xi_1-\xi_2)[2-j.\omega.T] + 2\xi_1 + j.\omega.T.\xi_2}{2-j.\omega.T}$$

$$z - \frac{1}{2}.(\xi_1-\xi_2) = \frac{\xi_2 - \xi_1 - \frac{\xi_1}{2}.j.\omega.T + \frac{\xi_2}{2}.j.\omega.T + 2\xi_1 + \xi_2 j.\omega.T.\xi}{2-j.\omega.T}$$

$$z - \frac{1}{2}.(\xi_1-\xi_2) = \frac{\xi_1+\xi_2+j.\omega.T.\frac{1}{2}.(\xi_1+\xi_2)}{2-j.\omega.T}$$

$$z - \frac{1}{2}.(\xi_1-\xi_2) = \frac{1}{2}.(\xi_1+\xi_2).\frac{2+j.\omega.T}{2-j.\omega.T}.\frac{2+j.\omega.T}{2+j.\omega.T}$$

$$z - \frac{1}{2}.(\xi_1-\xi_2) = \frac{1}{2}.(\xi_1+\xi_2).\frac{(2+j.\omega.T)^2}{4+(\omega.T)^2}$$

$$z - \frac{1}{2}.(\xi_1-\xi_2) = \frac{1}{2}.(\xi_1+\xi_2).\exp\left(j\tan^{-1}\left(\frac{4.\omega.T}{4-(\omega.T)^2}\right)\right) \qquad \text{(Eq.16)}$$

$$\left| z - \frac{1}{2}.(\xi_1 - \xi_2) \right| = \frac{1}{2}.(\xi_1 + \xi_2)$$

(Eq.17)

That it describes a family of circles inside the unit circle, with centers on the real axis.

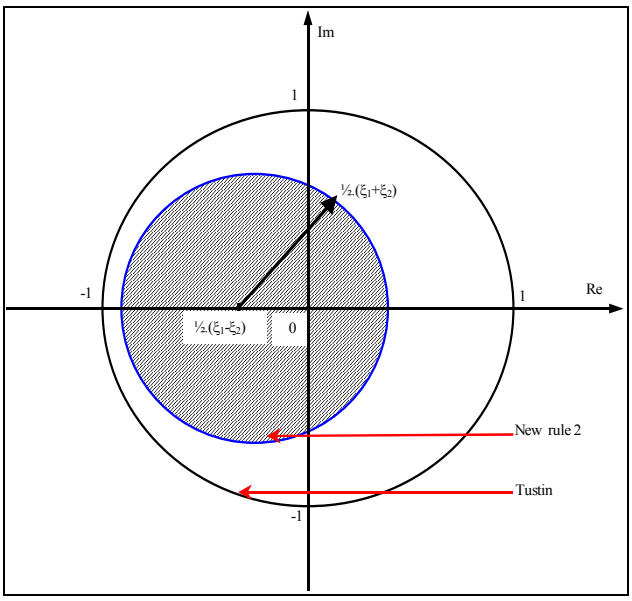

Figure 3- The new-rule 2 mapping.

We may note by the figures 2 and 3 that the Tustin, backward and new-rule 1 methods are particular cases of this new-rule 2.

PD CONTROL WITH THESE TRHEE RULES

Replacing the expression that governs the Tustin mapping in a PD control,

$$D(z) = k_p + k_d.s$$

(Eq.18)

we will have,

$$D(z) = \left(k_p + \frac{2.k_d}{T} \right).\frac{z + \left(\frac{k_p.T - 2.k_d}{k_p.T + 2.k_d} \right)}{z+1} \qquad \text{(Eq.19)}$$

A PD controller designed by new-rule 1 is given by:

$$D(z) = PD_{control} = \left(k_p + \frac{2.k_d}{T} \right).\frac{z + \left(\frac{k_p.T.\xi - 2.k_d}{k_p.T + 2.k_d} \right)}{z + \xi} \qquad \text{(Eq.20)}$$

A PD controller designed by the most general, than the last two, new-rule 2 is given by:

$$D(z) = PD_{control} = \left(k_p + \frac{2.k_d}{T} \right).\frac{z + \left(\frac{k_p.T.\xi_2 - 2.k_d.\xi_1}{k_p.T + 2.k_d} \right)}{z + \xi_2} \qquad \text{(Eq.21)}$$

NUMERICAL RESULTS

We have used the constant values showed in Table I in all simulations.

Table I: constants used.

Damping ratio ζ	0.9
Natural frequency ω_N	0.3 Hz
Proportional Gain Kp	3.0
Derivative Gain	4.8
New-Rule 1 coefficient ξ	0.1
New-Rule 2 coefficient ξ_1	0.8
New-Rule 2 coefficient ξ_2	0.1

In Table II we may see some numerical simulations done by a simulation tool running in a personal computer (Pentium IV, 500 MHz).

In the figures 4 to 7 we have a comparative results using many values for the sampling period T for the three rules: Tustin, New-Rule 1 and New-Rule 2.

Table II: numerical results obtained.

Sampling Period T in seconds	Mapping Rule	Stable	Unstable
0.35	Tustin	*	
	New-Rule 1	*	
	New-Rule 2	*	
0.7	Tustin		*
	New-Rule 1	*	
	New-Rule 2	*	
1.0	Tustin		*
	New-Rule 1	*	
	New-Rule 2	*	
1.2	Tustin		*
	New-Rule 1	*	
	New-Rule 2	*	
1.6	Tustin		*
	New-Rule 1	*	
	New-Rule 2	*	

3.0	Tustin		*
	New-Rule 1	*	
	New-Rule 2	*	
4.0	Tustin		*
	New-Rule 1	*	
	New-Rule 2	*	
4.5	Tustin		*
	New-Rule 1		*
	New-Rule 2		*

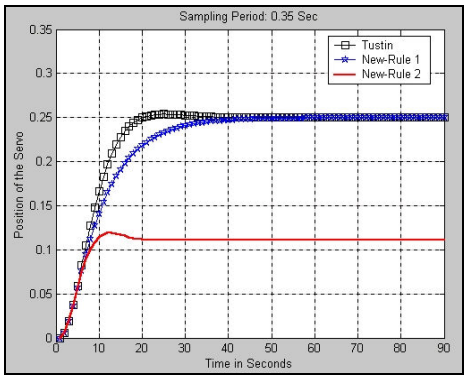

Figure 4- Numerical Results for T = 0.35 second.

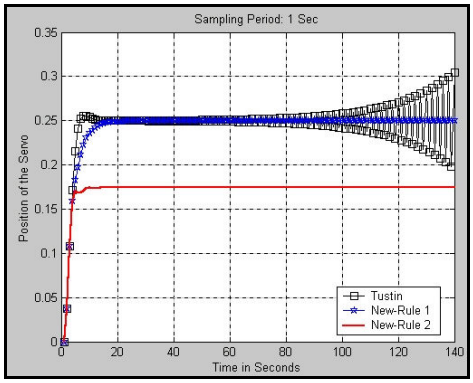

Figure 5- Numerical Results for T = 1.0 second.

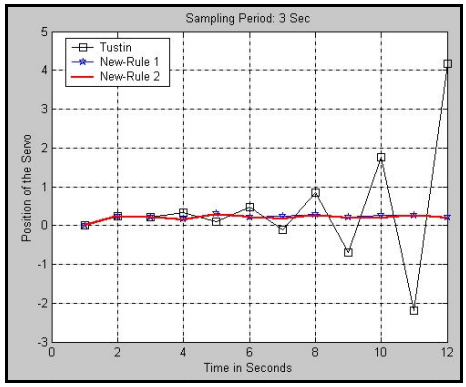

Figure 6- Numerical Results for T = 3.0 seconds.

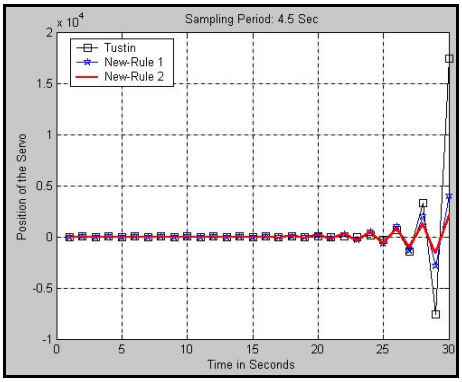

Figure 7- Numerical Results for T = 4.5 seconds.

CONCLUSION

We may note from the Table II and the figures 4-7 that the New-Rule 1 and New-Rule 2 are more robust to the aliasing phenomenon due the increasing of the sampling period T that the classical Tustin rule. In special, the New-Rule 2 responds to the input unit step with less power than the New-Rule 1. All of these effects were experimentally showed in this work but until now we do not have a concrete explanation for the phenomenon. A dedicated work is in course to investigate in details why these variations of the Tustin mapping becomes more robust to the aliasing and trying to bring a general and complete comprehension of this questions.

REFERENCES

[1] Tredinnick, M.R.AC.T. *The Presence of Bifurcation in a Closed-Loop Discrete Control of a Flexible Benchmark Plant analyzed from the Jury Stability Criterion*. SAE Brazilian Congress, November 2001.

[2] Tredinnick, M.R.A.C. *Controle Discreto da Atitude de Satélites Artificiais com Apêndices Flexíveis*. INPE – National Institute for Space Research. (Master Thesis). São José dos Campos, Brasil. Feb. 26, 1999.

[3] Franklin, G.F.; Powell, D. *Digital control of dynamic systems*. Reading: Addison-Wesley, 1981.

[4] Katz, P. *Digital control using microprocessors*. Englewood Cliffs: Prentice-Hall, 1981.

[5] Jury, E.I. *Theory and Application of the Z-Transform Method*. Robert Krieger Publishing Co., Inc., 1964.

[6] Houpis, C.H. and Lamont, G.B. *Digital Control Systems – Theory, Hardware, Software*. McGraw-Hill, 1985.

[7] Phillips, C.L. and Nagle, H. T. *Digital Control System Analysis and Design*. Prentice Hall International, 1995.

[8] Muth, E. J. *Transform Methods with Applications to Engineering and Operations Research*. Englewood Cliffs, 1977.

[9] Chen, C.T. Control System Design: Transfer-Function, State-Space and Algebraic Methods. Saunders College Publishing, 1993.

[10] Lam, H.Y.F. Analog and Digital Filters- Design and Realization. Prentice-Hall, 1979.

[11] Rao, G.V. Complex Digital Control Systems. Van Nostrand Reinhold Company, 1979.

[12] D'azzo, J.J. and Houpis, C. H. Linear Control System Analysis and Design – Conventional and Modern. McGraw-Hill, 1981.

[13] Junkins, J.L.; Kim, Y. *Introduction to dynamics and control of flexible structures*. Washington: AIAA, 1993. 444p. (AIAA Educational Series).

[14] Oppenheim, A.V. and Schafer, R.W. *Digital Signal Processing*. Prentice Hall, 1975.

[15] Silva, A. R. and Souza, L.C.G.; *Control System Flexible Satellite Interaction During Orbit Transfer Manoeuvre.* Advances in the Astronautical Sciences, Vol. 100 Part I, pp. 541-550. Spaceflight Dynamics 1998. ISBN 0-87703-453-2.

[16] Souza, L.C.G. and Silva, S. A . *Large Space Structure Vibration Control During Attitude Manoeuvre*. RBCM – J. of the Braz. Soc. Mechanical Sciences, Vol. XXI – Special Issue, pp. 542-551, 1999. ISSN0100-7386.

[17] Huntress, W.T. *Nasa's space science program: our outlook for the new millennium*. AAS – Strengthening Cooperation in the 21st Century, San Diego, 1996. USA: San Diego, 1996; p.3-30.

[18] Wie, B. *Space Vehicle Dynamics and Control*. AIAA Education Series. USA, 1998.

[19] Bryson, A. E. Jr. *Control of Spacecraft and Aircraft*. Princeton University Press, EUA, 1994.